MEMORANDUM
RM-5660-PR
JANUARY 1969

THE EFFECT OF STRESS-WAVE DIFFRACTION ON STRESS MEASUREMENTS AND A CONCEPT FOR AN OMNIDIRECTIONAL DYNAMIC STRESS GAGE

F. C. Moon and C. C. Mow

PREPARED FOR:

UNITED STATES AIR FORCE PROJECT RAND

The RAND Corporation
SANTA MONICA • CALIFORNIA

MEMORANDUM
RM-5860-PR
JANUARY 1969

THE EFFECT OF STRESS-WAVE DIFFRACTION ON STRESS MEASUREMENTS AND A CONCEPT FOR AN OMNIDIRECTIONAL DYNAMIC STRESS GAGE

F. C. Moon and C. C. Mow

This research is supported by the United States Air Force under Project RAND—Contract No. F44620-67-C-0015—monitored by the Directorate of Operational Requirements and Development Plans, Deputy Chief of Staff, Research and Development, Hq USAF. Views or conclusions contained in this study should not be interpreted as representing the official opinion or policy of the United States Air Force.

The RAND Corporation
1700 MAIN ST. • SANTA MONICA • CALIFORNIA • 90406

This study is presented as a competent treatment of the subject, worthy of publication. The Rand Corporation vouches for the quality of the research, without necessarily endorsing the opinions and conclusions of the authors.

Published by The RAND Corporation

PREFACE

The research reported in this Memorandum is a part of a continuing investigation of the effects of ground shock on underground structures. This study was prompted in general by a questioning of the accuracy of free-field stress measurements, and in particular by an interest in the effects of gage design on these measurements. Most of the current free-field stress data available are derived from particle-velocity measurements; very few are obtained through actual stress gages, a long-recognized inadequacy.

It is therefore the purpose of the Memorandum to investigate the feasibility of an omnidirectional stress gage and to provide theoretical background for the design and use of such a device.

Doctor F. C. Moon is presently affiliated with Princeton University and is also a consultant to the RAND Corporation.

SUMMARY

This Memorandum presents an analysis of the transient response of the pressure in an embedded elastic inclusion due to an incident compressional wave. It represents a continuing effort at RAND to evaluate transducer diffraction effects on ground stress-wave measurements. Included is an outline of a design for an omnidirectional pressure transducer with a response capable of being interpreted in terms of the theoretical solution presented in this Memorandum.

Both the frequency response and transient behavior are treated. It is found that the pressure or mean stress at the center of the inclusion will be insensitive to the curvature of the incident wave. The primary source of distortion between the inclusion pressure and the free-field pressure in the incident wave is internal reflections in the inclusion. An early time analysis reveals that these can be minimized by matching the acoustic impedance (product of density and compressional wave speed) of the inclusion with that of the matrix. An estimate of the time for these reflections to decay due to radiation "damping" is found to depend on the impedance ratio.

Two methods are presented for obtaining the total pressure response due to a nonperiodic incident wave. The first uses the calculus of residues and the high-frequency response to sum the resulting infinite series. The second method proceeds by solving the inverse problem: to find the incident wave pressure in terms of the inclusion pressure. This latter method is presented in the form of an integral equation for the inclusion pressure which enables an exact explicit solution to be found between successive reflections.

ACKNOWLEDGMENT

The authors wish to acknowledge Miss Tiina Repnau for her help in programming most of the numerical work.

CONTENTS

FIGURES

SYMBOLS

a = radius of inclusion

$\bar{B}$ = ratio of bulk moduli ($\bar{B} = B_1/B_2$)

$\bar{c}$ = ratio of compressional-wave speeds ($\bar{c} = c_{d1}/c_{d2}$)

$F[\ ]$ = Fourier transform

$j_n(x)$ = spherical Bessel functions

k = ratio of compressional-wave speed to shear-wave speed ($k = c_d/c_s$)

$L[\ ]$ = Laplace transform

P = pressure at center of inclusion

P_c = pressure in incident compressional wave

$P_n(x)$ = Legendre polynomials

t = time

α = normalized frequency ($\alpha = \omega a/c_{d1}$)

γ = negative imaginary part of normalized frequency

$\bar{\mu}$ = ratio of shear moduli ($\bar{\mu} = \mu_1/\mu_2$)

$\bar{\rho}$ = ratio of mass densities ($\bar{\rho} = \rho_1/\rho_2$)

τ = time normalized with respect to half transit time ($\tau = tc_{d1}/a$)

Ω = real part of normalized frequency

ω = circular frequency

Subscripts

1 = matrix material

2 = inclusion material

I. INTRODUCTION

Among the many effects associated with a nuclear-explosion-induced ground shock that must be considered in the design of a survivable system is the magnitude of the stress in the ground shock. In fact, most design specifications of a hardened system usually call for structures to withstand a certain stress level. Thus the abilities to predict and to measure free-field stress are of prime importance in any nuclear effects tests.

Most of the existing stress gages are devised primarily for static measurements and may not be applied to dynamic stress measurement.[1] There have been many recent studies attempting to produce better stress gages capable of measuring high-intensity ground stress, but usually because of their complex geometric shape, a precise analysis of the wave-transducer interaction is impossible; hence, the interpretation of data is in doubt.[1] A strain-sensitive transducer of simple shape and construction is needed, with a response capable of being analyzed by the methods of the theory of elastic wave propagation and diffraction.

A transducer to measure ground stresses should have the following characteristics:

1. The strength to withstand high stresses
2. Elastic properties to produce measurable strains
3. Ease of installation and recoverability
4. Insensitivity to orientation
5. Small rise time, minimized overshoot, and large internal transient decay
6. Compatibility with standard auxiliary equipment

The transducer we propose to examine is an elastic spherical inclusion to be buried in the ground, and sensitive, through strain gages, to the mean stress or pressure at its origin. Such a device is insensitive to its angular orientation both because of its symmetry and because of the scalar nature of the mean stress or pressure. As our first task we will examine the response characteristics of such an inclusion.

o meet the requirement of high strength, the material of the sphere will most likely have elastic properties different from those of the ground material. Hence, diffraction effects are likely, and their effect on the response of the transducer should be examined. Toward this end we treat the problem of the diffraction of a transient compressional pulse by an elastic isotropic spherical inclusion bonded to an infinite elastic isotropic matrix. Then some design criteria are presented for the selection of the material, size, and response times of a spherical strain transducer.

II. FREQUENCY RESPONSE OF AN ELASTIC INCLUSION

The study of the response of an elastic inclusion has received much attention in the last decade. These studies have dealt mainly with harmonic compressional waves.[2,3] Recently, however, Mow[4,5] has examined the transient behavior of a rigid inclusion and has correlated the separate displacements of the inclusion and the ground. He found that the inclusion and free-field displacements could diverge at early times even for equal densities, satisfying an essential criterion of field testing. Similarly the stresses in an elastic inclusion are expected to differ in both magnitude and phase from those in the free field. The extent of this divergence and the factors that will minimize it are discussed below.

BASIC EQUATIONS

Since the harmonic solution has been discussed elsewhere,[3] we will only briefly review the relevant equations.

We suppose both the inclusion and matrix to be homogeneous, isotropic, linearly elastic mediums in which the usual stress-strain relationships hold. For each material there are two elastic constants and two wave speeds: a compressional or longitudinal wave c_d, and a shear or transverse wave c_s.

Outside the inclusion we imagine a source of either plane or spherical harmonic compressional waves with a displacement potential given by

$$\phi^P = \Phi_0 e^{i\omega(z-c_{dl}t)/c_{dl}} \qquad \text{plane wave} \qquad (1)$$

$$\phi^S = \frac{S_0 e^{i\omega(R-c_{dl}t)/c_{dl}}}{R} \qquad \text{spherical wave} \qquad (2)$$

$$\underline{u} = \nabla\Phi \qquad (3)$$

where z is an axial coordinate (Fig. 1), R is the distance from the source to the field point, and $\underline{u}$ is the displacement. The potentials

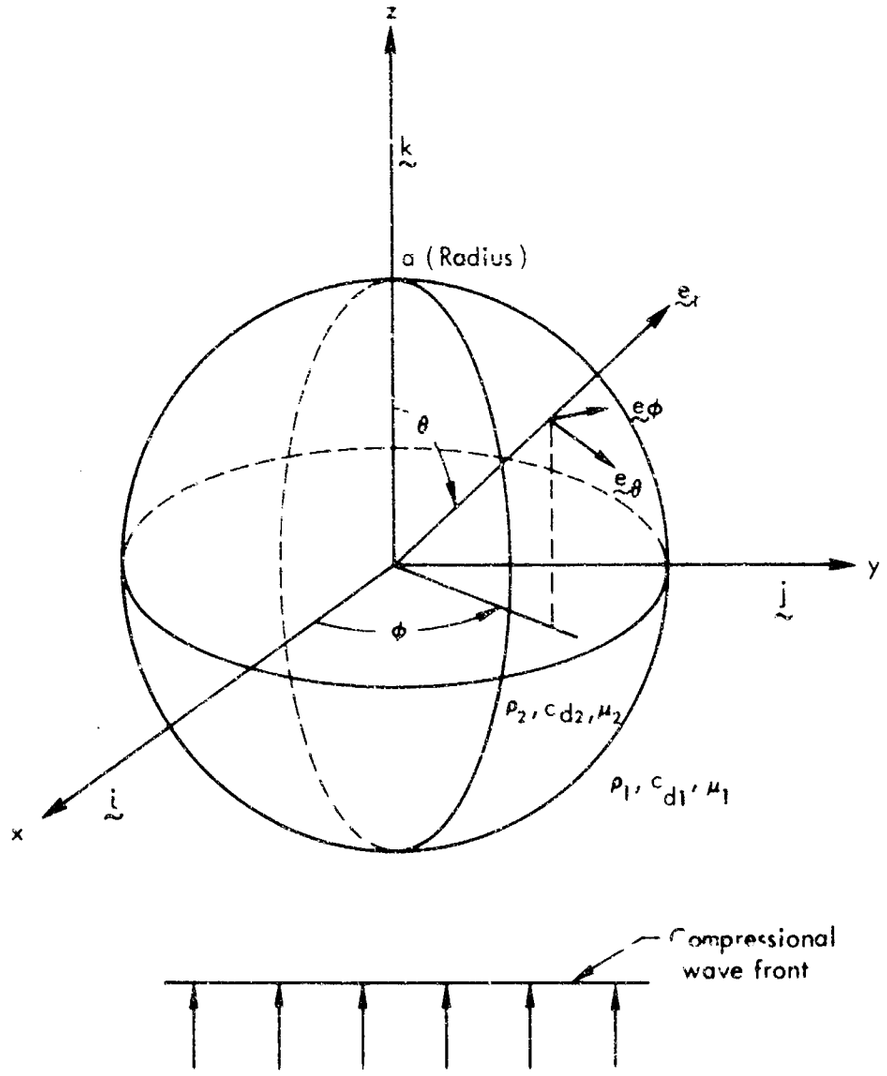

Fig. 1 — Geometry of spherical inclusion

represented by Eqs. (1) and (2) give the displacement in a medium without an inclusion. The presence of the inclusion will scatter waves into the medium and refract waves into the inclusion. The scattered and refracted fields will contain both compressional and transverse waves.

Inside the inclusion the motion is of the form of standing waves or vibrations, and the refracted displacement potentials take the form,[3]

$$\left.\begin{aligned} \underline{u} &= \nabla\phi + \nabla \times (e_\phi \partial\Psi/\partial\theta) \\ \phi &= -\sum_{n=0}^{\infty} C_n j_n(\omega r/c_{d2}) P_n(\cos\theta) \\ \Psi &= -\sum_{n=0}^{\infty} D_n j_n(\omega r/c_{s2}) P_n(\cos\theta) \end{aligned}\right\} \qquad (4)$$

where $j_n(\alpha)$ are spherical Bessel functions and $P_n(x)$ are Legendre polynomials.[6]

AVERAGE AND CENTROIDAL STRESSES AND DISPLACEMENT

The induced stresses are derived from Eq. (4) using the generalized Hooke's Law and have been tabulated by Pao and Mow.[3] The stresses and displacements depend on all the excited modes in the inclusion. However, if the inclusion is being used as a transducer, then knowledge of the stresses at one point will be sufficient. The most logical point to examine is the origin.

Using the small-argument limit for the spherical Bessel functions,[6]

$$j_n(\alpha)_{\alpha\to 0} \rightarrow \frac{\alpha^n}{1.3.5 \ldots (2n+1)}$$

the displacement and stresses at the origin become

$$u_z = -\frac{\omega}{3c_{d1}}\,(C_1 - 2k_2 D_1) \tag{5}$$

$$\left.\begin{aligned} \tau_{zz} &= -P + 2S \\ \tau_{xx} &= \tau_{yy} = -P - S \\ P &\equiv -1/3\,(\tau_{xx} + \tau_{yy} + \tau_{zz}) = -B_2 \frac{\omega^2}{c_{d2}^2} C_0 \\ S &\equiv \frac{2\mu_2}{5}\left(\frac{\omega}{c_{d2}}\right)^2 \left(\frac{C_2}{3} - k_2^2 D_2\right) \end{aligned}\right\} \tag{6}$$

where $k_2 = c_{d2}/c_{s2}$ is the ratio of compressional-wave speed to shear-wave speed in the inclusion. Thus the displacement at the origin depends only on the first dilatational and shear modes. The mean pressure P at the origin depends only on the symmetrical modes, and the maximum shear stress 3S/2 depends solely on the vibratory modes associated with C_2 and D_2.

Similar remarks apply for the average displacement or motion of the center of mass of the inclusion and average pressure over the entire sphere, i.e.,

$$\langle \underline{u} \rangle = -\underline{e}_z \left(\frac{\omega}{c_{d2}}\right) \frac{1}{\alpha_2} \left[C_1 j_1(\alpha_2) - 2D_1 j_1(\beta_2)\right] \tag{7}$$

$$\langle P \rangle \equiv \langle -B_2 \nabla \cdot \underline{u} \rangle = -B_2 \left(\frac{\omega}{c_{d2}}\right) \frac{2j_1(\alpha_2)}{\alpha_2} C_0 \tag{8}$$

where $\alpha_2 = \bar{c}\alpha = \omega a/c_{d2}$ and $\beta_2 = \omega a/c_{s2}$.

It is evident that the behavior of either the stresses at the origin or the average mean pressure depends only on the frequency response of the coefficients C_0, C_2, and D_2. These coefficients are determined

from the boundary conditions. For a bonded inclusion, the boundary conditions require continuity of stress and displacement, i.e.,

$$\left.\begin{aligned} u_r^{(s)} + u_r^{(I)} &= u_r^{(r)} \\ u_\theta^{(s)} + u_\theta^{(I)} &= u_\theta^{(r)} \\ \tau_{rr}^{(s)} + \tau_{rr}^{(I)} &= \tau_{rr}^{(r)} \\ \tau_{r\theta}^{(s)} + \tau_{r\theta}^{(I)} &= \tau_{r\theta}^{(r)} \end{aligned}\right\} \quad \text{on } r = a \tag{9}$$

where s, I, and r indicate "scattered," "incident," and "refracted," respectively.* For our purposes, it is sufficient to know that C_0 depends only on the first and third boundary conditions of Eq. (9). That is, the pressure at the origin or the average pressure over the entire inclusion does not depend on whether the tangential displacements or shear stresses at the interface are continuous. Thus the same value of C_0 will result if "slipping" boundary conditions of zero shear stress on the interface are applied.

$$\left.\begin{aligned} u_r^{(s)} + u_r^{(I)} &= u_r^{(r)} \\ \tau_{rr}^{(s)} + \tau_{rr}^{(I)} &= \tau_{rr}^{(r)} \\ \tau_{r\theta}^{(s)} + \tau_{r\theta}^{(I)} &= 0 \\ 0 &= \tau_{r\theta}^{(r)} \end{aligned}\right\} \quad \text{on } r = a \tag{10}$$

The induced pressure at the center of our transducer inclusion will thus be insensitive to the bonding or grouting as long as the matrix

*These equations are given in a more explicit form in Ref. 3.

makes normal contact with the sphere. For this reason, we study only the frequency and transient response of the mean pressure at the origin of the inclusion. The coefficient C_0 is given by the expression[3]

$$C_0 = -N_0 i\alpha e^{i\alpha}\left\{\frac{1}{\rho c}\alpha(\alpha+i)j_0(\bar{c}\alpha) - \left[\frac{4(1-\bar{\nu})}{\bar{\mu}k_1^2}(\alpha+i)+i\alpha^2\right]j_1(\bar{c}\alpha)\right\}^{-1} \tag{11}$$

where

$$N_0 = \begin{cases} \Phi_0 & \text{plane wave} \\ S_0 \frac{i\alpha}{a} h_0\left(\frac{\alpha d}{a}\right) & \text{spherical wave} \end{cases}$$

where d is the distance from the wave source to the inclusion center, and $h_0(x)$ is the zero-order spherical Hankel function.

Let us next examine the consequences of choosing either a plane or a curved incident compressional wave. The mean pressure due to the incident wave is given in the two cases by

$$P_c = -B_1 \nabla\cdot\underline{u}^{(I)} = -B_1 \nabla^2\phi^{(I)} = -\frac{B_1}{c_{d1}^2}\frac{\partial^2\phi}{\partial t^2} \tag{12}$$

where Φ satisfies the wave equation.[6] Substituting Eqs. (1) and (2) into the above gives

$$P_c = B_1\left(\frac{\omega}{c_{d1}}\right)^2 \begin{cases} \Phi_0 & \text{plane wave} \quad (13a) \\ S_0 \frac{i\alpha}{a} h_0\left(\frac{\alpha d}{a}\right) & \text{spherical wave} \quad (13b) \end{cases}$$

where $h_0(x) = e^{ix}/ix$.

Comparing Eqs. (13a) and (13b),[6] we find that the relationship between the incident pressure and inclusion pressure is the same, i.e.,

$$\left.\begin{aligned} P(\alpha) &= P_c \frac{\bar{c}}{\bar{B}} \frac{i\alpha e^{-i\alpha}}{H(\alpha)} \equiv A(\alpha)P_c \\ H(\alpha) &= \left\{ \frac{1}{\bar{\rho}\bar{c}} \alpha(\alpha + i) j_0(\bar{c}\alpha) - \left[\frac{4(1 - \bar{\mu})}{\bar{\mu}k_1^2} (\alpha + i) + i\alpha^2 \right] j_1(\bar{c}\alpha) \right\} \end{aligned}\right\} \quad (14)$$

We need no longer distinguish between spherical or plane waves, since the response is identical in both cases. The same can be said for the displacement and shear stress. In fact, as long as a quantity depends on only one mode, the relation between its value inside and its value in the free field remains the same whether the incident wave is plane, spherical, or generally dilatational. However, for a quantity such as τ_{zz}, the axial stress which depends on the zeroth and second modes, this is not true; i.e., if

$$\tau_{zz}(\underline{r} = 0) = \tau_{zz}^I g_p(\omega) \qquad \text{plane wave}$$

$$\tau_{zz}(\underline{r} = 0) = \tau_{zz}^I g_s(\omega) \qquad \text{spherical wave}$$

then $g_p(\omega) \neq g_s(\omega)$. This gives further impetus to studying the mean pressure P rather than, for example, the axial stress τ_{zz}.

Examining the frequency response for the mean pressure at the origin, we observe that at low frequencies, i.e., $\omega \to 0$, $\alpha \to 0$

$$j_0(\bar{c}\alpha) \to 1, \qquad j_1(\bar{c}\alpha) \to \alpha/3$$

$$P \underset{\omega \to 0}{\to} P_c \frac{\bar{c}}{\bar{B}} \left[\frac{1}{\bar{\rho}\bar{c}} - \frac{4}{3} \frac{(1 - \bar{\mu})}{\bar{\mu}k_1^2} \bar{c} \right]^{-1} \quad (15)$$

This limit yields the same pressure as the static problem of a spherical elastic inclusion embedded in an elastic matrix with hydrostatic

pressure P_c at infinity.[7] The ratio of output to input P/P_c is a constant at low frequencies and can be called an amplification or gain factor A_0. The gain factor is presented in Table 1 for different inclusion materials in a granite matrix. At high frequencies

$$P(\alpha) \underset{\alpha\to\infty}{\to} P_c \frac{\bar{\rho}(\bar{c})^3}{\bar{B}} \bar{e}^{i\alpha}(\overline{\rho c}\cos \bar{c}\alpha - i \sin \bar{c}\alpha)^{-1} \tag{16}$$

The product $\overline{\rho c}$ is called the impedance ratio, and its departure from unity gives a clue to the nature of the reflection of dilatation waves from the boundary separating two media. If $\overline{\rho c} = 1$, the gain is again constant, whereas if the impedance ratio departs from unity, the denominator has periodic maxima and minima. Thus the gain exhibits resonance peaks with frequency, or the internal reflections reinforce one another at certain frequencies. The resonances at large frequency are easily found: for $\overline{\rho c} > 1$, $\bar{c}\alpha = n\pi/2$, and n an odd number,

$$(P/P_c)\max = \bar{\rho}(\bar{c})^3/\bar{B} \tag{17a}$$

and for $\overline{\rho c} < 1$, $\bar{c}\alpha = n\pi/2$, and n an even number,

$$(P/P_c)\max = \bar{c}^2/\bar{B} \tag{17b}$$

The frequency response curves using the exact relation Eq. (14) are shown in Figs. 2* through 5. They show the resonances at the proper frequencies when α is large. Values obtained previously check the computed maxima of these curves.

An ideal transducer is one for which the gain or amplification factor is independent of frequency. Thus for measurement of elastic waves in granite, aluminum or titanium would make a better transducer than plastic or lead, for example (Figs. 2 through 5). Furthermore, we can say that unless the matrix and inclusion transducer are "matched" ($\overline{\rho c} = 1$), the internal reflections can mask the incident signal.

*For discussion of Cases A and B in Fig. 2, see page 20 and Table 2.

Table 1

TRANSIENT RESPONSE CHARACTERISTICS OF DIFFERENT INCLUSION MATERIALS IN A GRANITE[a] MATRIX

Inclusion Material	Impedance Ratio $\overline{\rho c}$	Compression-Wave Speed Ratio $\bar{c}$	C_{d2}/C_{s2}	Strain Amplification Static Limit $A_o\bar{B}$	Strain Amplification High Frequency $(\bar{c})^2$	Overshoot of High-Frequency Limit (percent)	"Damping Time" γ_o^{-1} (units of half transit time)
Steel	0.356	1.07	1.87	0.483	1.14	....	2.87
Titanium	0.595	1.02	1.94	0.662	1.04	....	1.48
Lead	0.725	3.15	2.84	1.25	9.92	....	3.43
Aluminum	0.941	0.962	2.11	0.834	0.925	....	0.545
Magnesium	1.63	1.07	1.89	1.26	1.15	23.8	1.50
Lucite	5.16	2.31	2.44	2.00	5.34	67.4	11.7
Polyethylene	9.26	3.17	3.61	2.13	10.0	80.6	29.3

[a]Granite (Rockport, Mass., USA): $\rho_1 = 2.63$ gm/cm^3, $C_{d1} = 6.18$ km/sec, $C_{s1} = 3.54$ km/sec.[8] Similar data for inclusion materials taken from American Institute of Physics Handbook (2nd ed.).

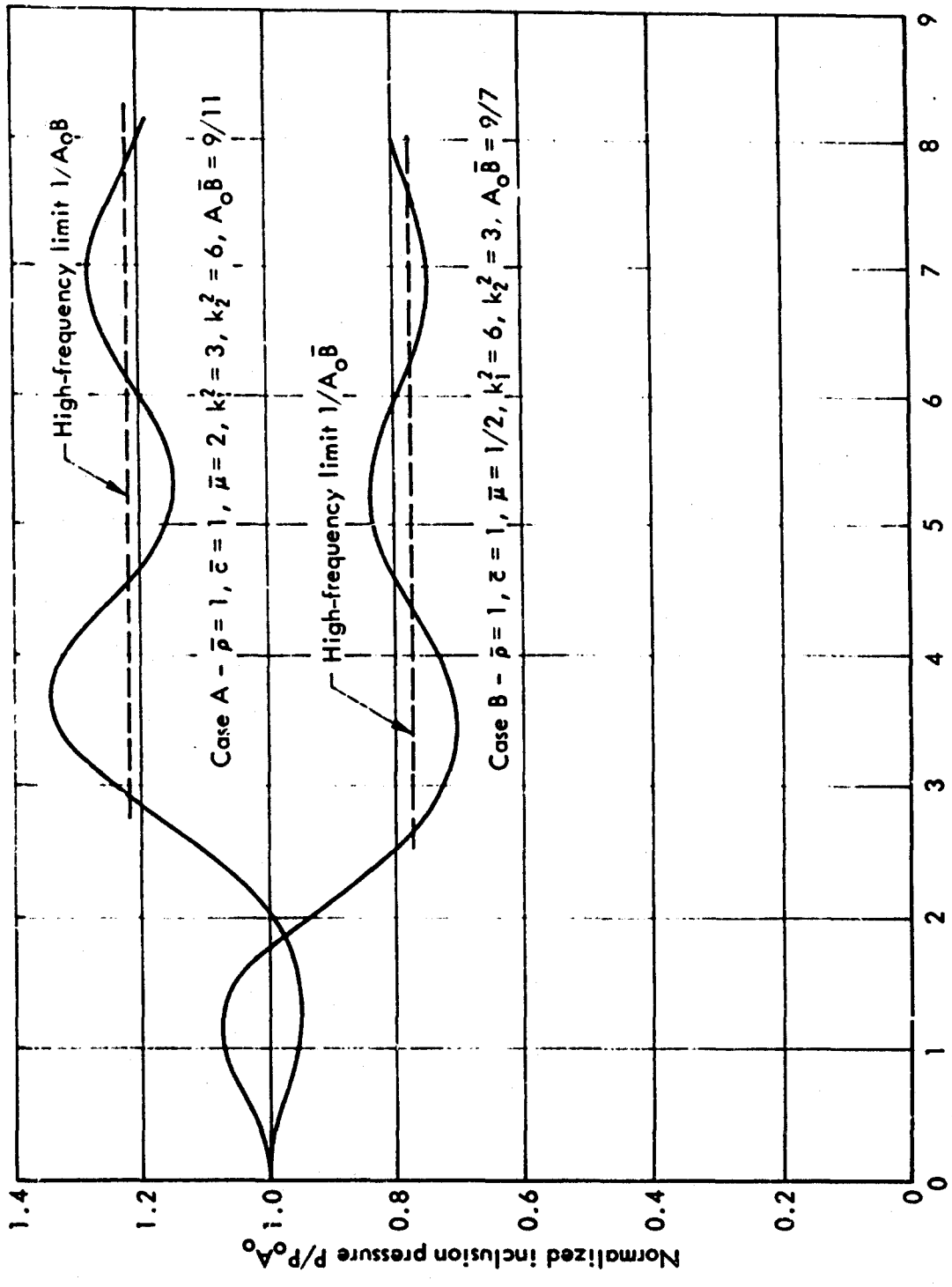

Fig. 2 — Frequency response of the pressure at the center of a spherical elastic inclusion in an infinite matrix; effect of mismatch of shear modulus

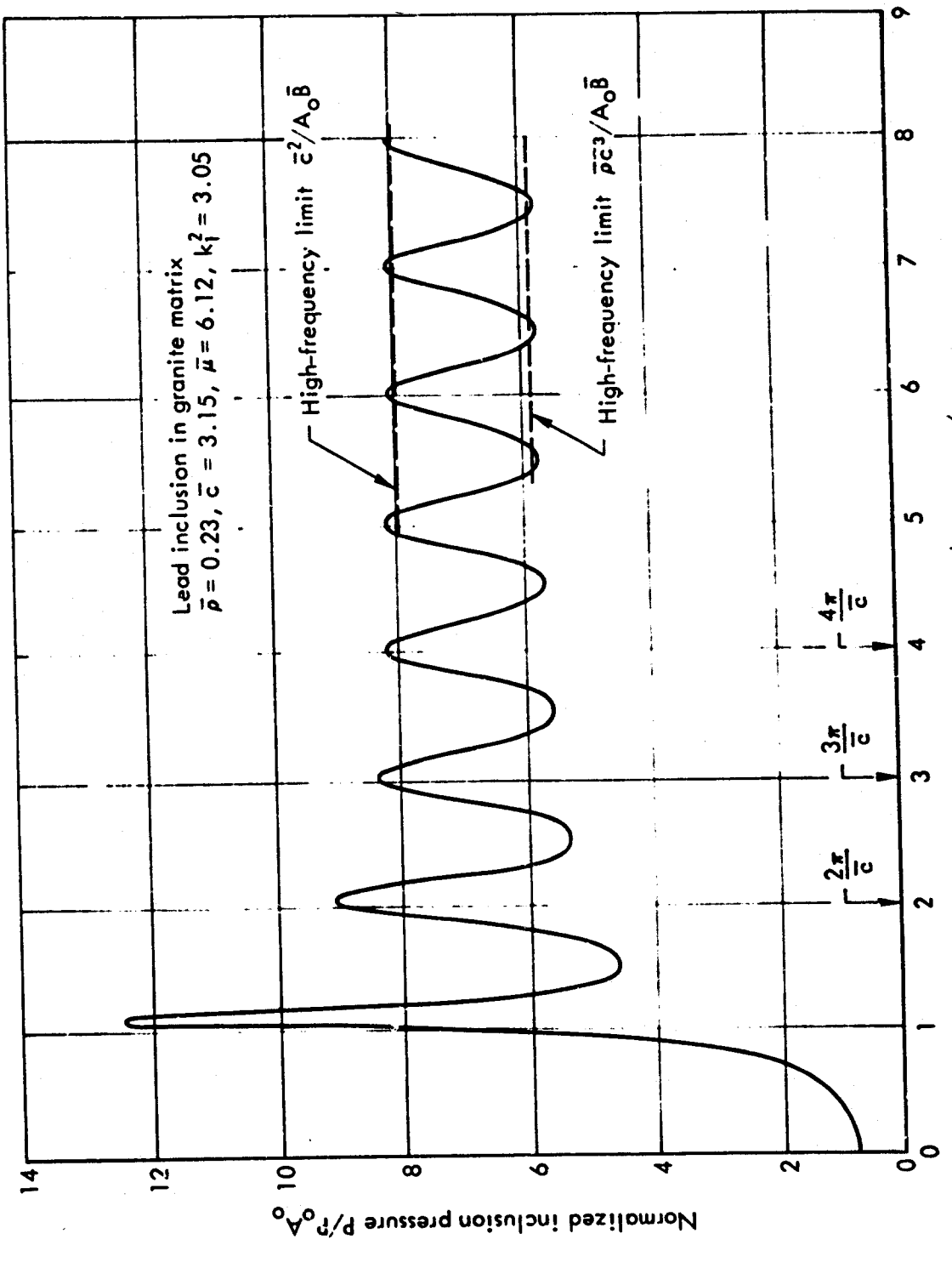

Fig. 3— Frequency response of the pressure in a lead inclusion in a granite matrix

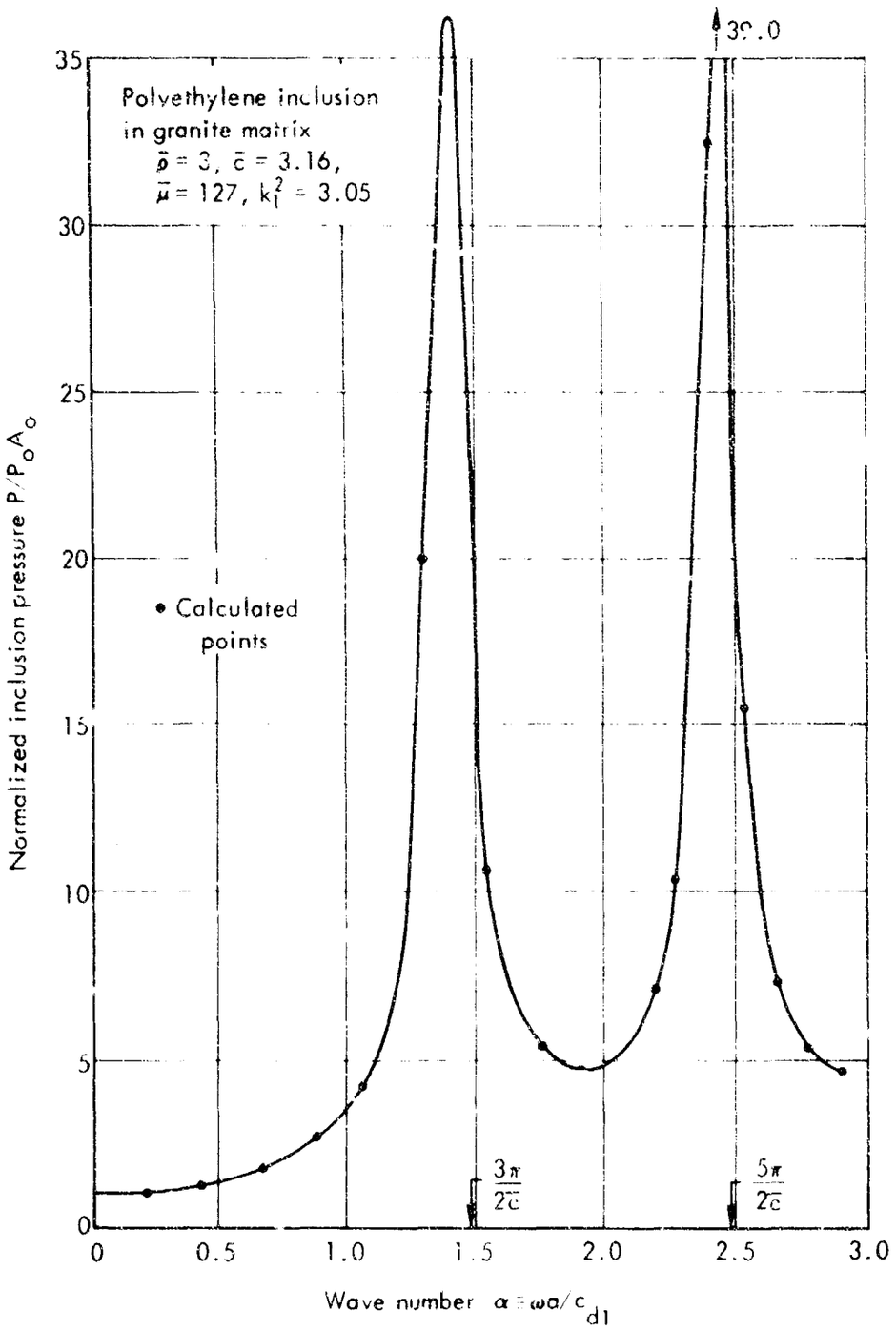

Fig. 4 — Frequency response of the pressure in a polyethylene inclusion in a granite matrix

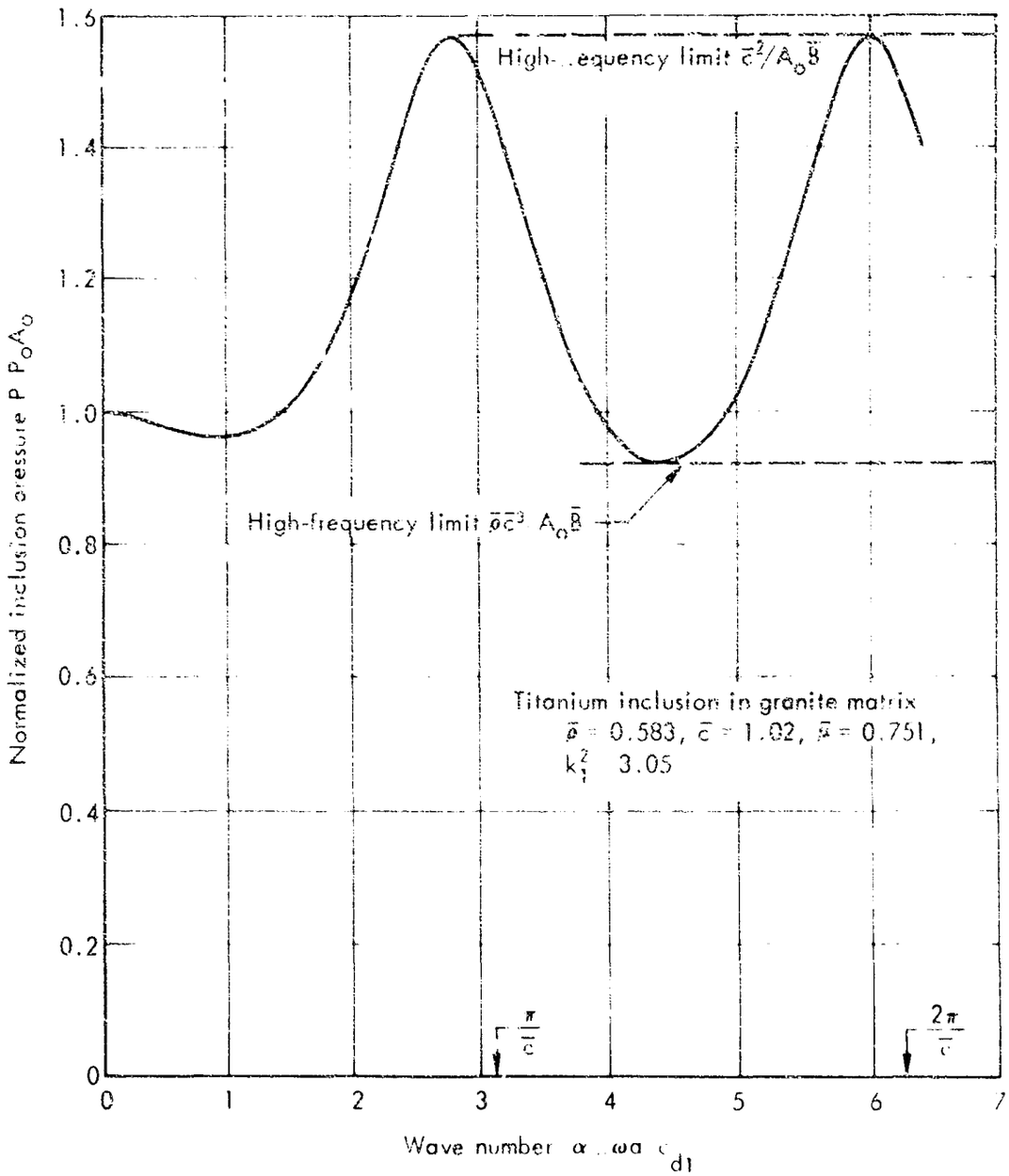

Fig. 5 — Frequency response of the pressure in a titanium inclusion in a granite matrix

III. TRANSIENT RESPONSE OF AN EMBEDDED ELASTIC INCLUSION

DIRECT PROBLEM

If the incident signal or pressure is nonperiodic, the inclusion pressure at the origin may be obtained as an inverse Fourier transform of the product of the gain $A(\alpha)$ (Eq. (14)) and the transform of the incident pressure,[9] i.e.,

$$\left.\begin{aligned} P(\tau) &= \frac{1}{2\pi}\int_{-\infty}^{\infty} A(\alpha)F[P_c(\tau)]e^{-i\alpha\tau}d\alpha \\ F[P_c(\tau)] &\equiv \int_{-\infty}^{\infty} P_c(\tau)e^{i\alpha\tau}d\tau \end{aligned}\right\} \qquad (18)$$

where $P_c(\tau)$ would be the pressure at the origin in the absence of the inclusion. The time τ is normalized by the time the incident wave transits half the inclusion, i.e., a/c_{d1}, and α is a nondimensional frequency.

Suppose $P_c(\tau)$ has the form

$$P_c(\tau) = \begin{cases} 0, & \tau < 0 \\ P_0 f(\tau), & \tau \geq 0 \end{cases}$$

where $f(\tau) \to e^{-\lambda\tau}$ as $\tau \to \infty$. In units of the half transit time a/c_{d1}, the pulse arrives at the inclusion surface at $\tau = -1$. The time for a compressional wave to transit the distance "a" in the inclusion material is $\bar{c}$. We should then expect the response

$$P(\tau) = 0$$

for $\tau < -1 + \bar{c}$.

To show that this is the case, the calculus of residues is used to evaluate Eq. (18) and to show that all poles of the integrand lie in the lower half of the complex plane. (See Fig. 6.) In the examination of the function $A(\alpha)$ in the complex α-plane, we note that the singularities are determined by:

$$\left.\begin{aligned} \text{Real } H(\alpha) &= 0 \\ \text{Im } H(\alpha) &= 0 \end{aligned}\right\} \tag{19}$$

It can be shown that the roots of Eq. (19) always come in pairs, i.e., if α is a root, $-\alpha^*$ is also a root.[†] To show that the imaginary part of the root is always negative, we note that as real $\alpha \to \infty$, where $\alpha = \Omega - i\gamma$, the equations for the roots of Eq. (19) take this form (where $H(\alpha)$ is given by Eq. (14)):

$$\cos \bar{c}\Omega(\overline{\rho c} \cosh \bar{c}\gamma - \sinh \bar{c}\gamma) = 0$$

$$\sin \bar{c}\Omega(\cosh \bar{c}\gamma - \overline{\rho c} \sinh \bar{c}\gamma) = 0$$

Thus the roots are determined by

$$\text{Case 1: } \overline{\rho c} < 1, \quad \sin \bar{c}\Omega = 0, \quad \bar{c}\Omega = n\pi/2, \quad n \text{ even}$$

$$\tanh \bar{c}\gamma_0 = \overline{\rho c}, \quad \gamma \equiv \gamma_0 \tag{20a}$$

$$\text{Case 2: } \overline{\rho c} > 1, \quad \cos \bar{c}\Omega = 0, \quad \bar{c}\Omega = n\pi 2, \quad n \text{ odd}$$

$$\tanh \bar{c}\gamma_0 = 1/\overline{\rho c} \tag{20b}$$

For high frequency, the radiation damping coefficient γ approaches a positive constant if $\overline{\rho c} \neq 1$.

[†]Asterisk indicates conjugate.

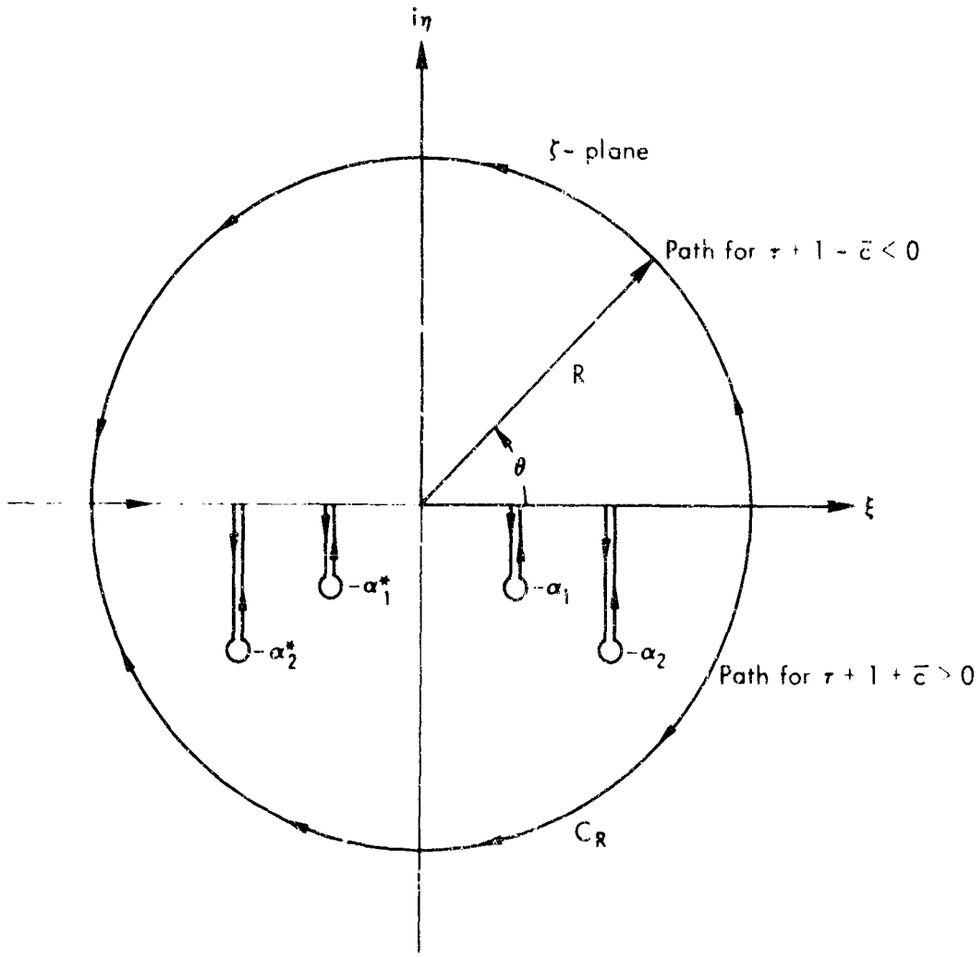

Fig. 6 — Path of integration in complex plane for the transient problem

Since Im $\alpha < 0$, there are no poles in the upper half plane, and substitution of Eq. (14) for $A(\alpha)$ into Eq. (18) reveals that $P(\tau) = 0$ for $\tau + 1 - \bar{c} < 0$, which agrees with our initial supposition.

For Im $\alpha < 0$

$$A(\alpha) \sim e^{-i(1-\bar{c})\alpha}$$

and $P(\tau)$ for $(\tau + 1 - \bar{c} > 0)$ is given by the sum of the residue of $A(\alpha)F[f]$ in the lower half plane.

For the special case of a step function,

$$f = e^{-\lambda\tau}, \qquad \lambda \to 0$$

it follows that

$$P(\tau) \to \begin{cases} 0, & \tau < -1 + \bar{c} \\ P_0\left[A_0 - \dfrac{2\bar{c}}{\bar{B}}\ \mathrm{Im}\sum_{j=1}^{x} \dfrac{e^{-(\gamma_j + i\Omega_j)(\tau+1)}}{H'(\alpha_j)}\right], & \tau > -1 + \bar{c} \end{cases} \tag{21}$$

where the sum is over the conjugate roots of $H(\alpha_j) = 0$ and the property $H'(-\alpha^*) = -H'^*(\alpha)$ has been taken into consideration.[+] For large j the roots take the form given in Eq. (20).

The first term in Eq. (21) is, to within a factor, the incident pressure. The second is a transient pressure due to diffraction and internal reflections. The maximum rate of decay of the transient is proportional to $e^{-\gamma_0\tau}$ where γ_0 is given by either Eq. (20a) or Eq. (20b). The normalized "damping" time is $1/\gamma_0$. For a granite matrix and aluminum inclusion this time is 1.5 half transit times, whereas for a plastic inclusion, $1/\gamma_0 = 30$ half transit times.

The complete solution may be obtained by using the first few roots of $H(\alpha) = 0$, found numerically until $\gamma_j \to \gamma_0$. The remaining terms in

[+] Prime sign indicates derivative.

the series, using the approximation Eq. (20) for α_j, constitute a Fourier series and may then be summed analytically.

As an illustration, consider the cases for which the frequency response is calculated in Fig. 2 (the upper curve is close to that for an aluminum inclusion in a granite matrix). In these cases the densities and compressional velocities are matched, but the shear speeds of inclusion and matrix are different, i.e., $\overline{\rho c} = 1$, $\bar{\mu} \neq 1$. The first few roots and residues for each case are presented in Table 2. We observe that the magnitudes of the third and fourth modes are about one-half of the first symmetric vibration mode of the inclusion in the matrix. The relative importance of the higher modes was also found by Skalak and Friedman[10] in studying the reflection of an acoustic step wave from an elastic cylindrical shell. We note also that the real parts of the roots came close to the peaks in the frequency response curves (Fig. 2).

The pressure response to an incident compressional step wave at the center of an aluminum inclusion in a granite matrix is given by

$$P(\tau) = P_0(22/9)\Big\{1 + (1.301)e^{-1.251(\tau+1)}\sin\left[3.532(\tau + 1) + \theta_1\right]$$

$$+ (0.8465)e^{-1.540(\tau+1)}\sin\left[6.839(\tau + 1) + \theta_2\right]$$

$$+ (0.6827)e^{-1.719(\tau+1)}\sin\left[10.04(\tau + 1) + \theta_3\right] + \ldots\Big\}$$

for $\tau > 0$.

This curve is plotted in Fig. 7, using only the first three modes. (Note that since $\overline{\rho c} = 1$, we cannot use Eq. (20) to analytically sum the rest of the terms in the series.) Even though the series converges slowly for any given time, the exponential radiation damping terms ensure that the transient will be negligible in a few transit times for this case.

Table 2

CALCULATED ROOTS AND RESIDUES FOR THE TRANSIENT RESPONSE OF AN INCLUSION TO AN INCIDENT-WAVE FIELD

n	$\alpha_n = \Omega - i\gamma_n$	$H'(\alpha)_n = a_n^{-1} e^{i\theta_n}$	
		a_n	θ_n
Case A:[a]	$\bar{\rho} = \bar{c} = 1$,	$\bar{\mu} = 2.0$,	$k_1^2 = 3.0$, $k_2^2 = 6.0$
1	3.532 - 1.251 i	0.5324	$\pi - \tan^{-1} 0.5785$
2	6.839 - 1.540 i	0.3463	$-\tan^{-1} 0.7803$
3	10.04 - 1.719 i	0.2793	$\pi - \tan^{-1} 0.8568$
Case B:[a]	$\bar{\rho} = \bar{c} = 1$,	$\bar{\mu} = 0.5$,	$k_1^2 = 6.0$, $k_2^2 = 3.0$
1	1.381 - 1.201 i	1.258	$\pi + \tan^{-1} 0.8828$
2	5.144 - 1.431 i	0.4087	$\tan^{-1} 1.225$
3	8.407 - 1.643 i	0.3071	$\pi + \tan^{-1} 1.116$
4	11.61 - 1.793 i	0.2582	$\tan^{-1} 1.073$

[a]See Fig. 2.

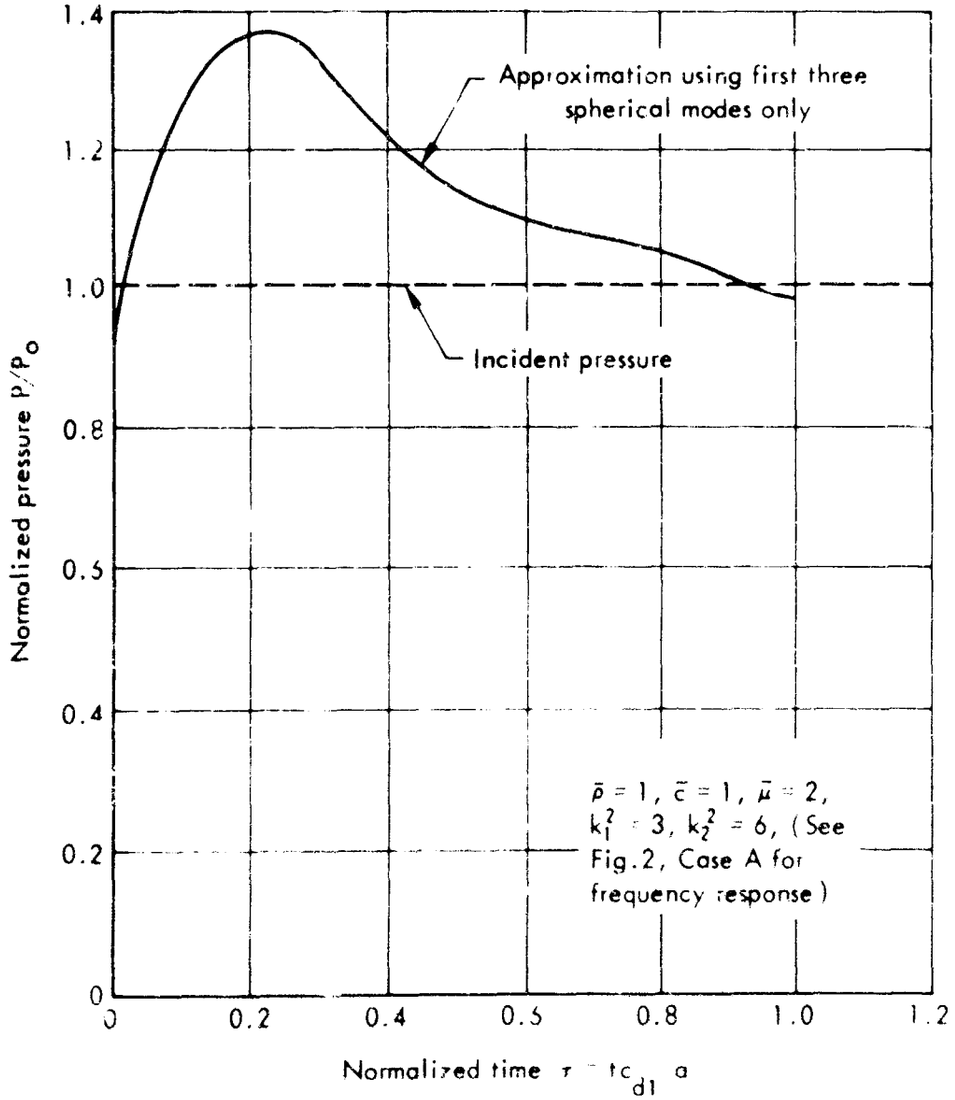

Fig. 7 — Transient response of the pressure in an aluminum inclusion in a granite matrix due to an incident compressional step wave

LARGE-TIME AND SMALL-TIME RESPONSE

Let us now examine the behavior of Eq. (18) for $\tau \to \infty$ or its equivalent $\alpha \to 0$. For this case $A(\alpha) \to A(0) \equiv A_0$, a constant, and the remaining integral is the inverse of F[f]

$$P(\tau) \underset{\tau\to\infty}{\to} A_0 P_c(\tau + 1) \tag{22}$$

(It should be noted that the phase of the right-hand term is arbitrary for $\tau \to \infty$.)

For small times we examine Eq. (14) under the limit $\alpha \to \infty$, for which Eq. (18) becomes

$$P(\tau) = \bar{\rho}\,\frac{(\bar{c})^3}{\bar{B}}\,\frac{1}{2\pi}\int_{-\infty}^{\infty}\frac{e^{-i\alpha(\tau+1)}F[f]d\alpha}{(\overline{\rho c}\cos\bar{c}\alpha - i\sin\bar{c}\alpha)} \tag{23}$$

This may be inverted if we rewrite Eq. (23) in the form of a Laplace transform, setting $\alpha = is$

$$P(\tau) = P_0\bar{\rho}\,\frac{(\bar{c})^3}{\bar{B}}\,\frac{1}{2\pi i}\int_{-i\infty}^{i\infty}\frac{e^{s(\tau+1)}L[f]ds}{(\overline{\rho c}\cosh\bar{c}s + \sinh\bar{c}s)} \tag{24}$$

or

$$P(\tau) = P_0\bar{\rho}\left(\frac{\bar{c}}{\bar{B}}\right)^3 \sinh\bar{c}\gamma_0\,\frac{1}{2\pi i}\int_{-i\infty}^{i\infty}\frac{e^{s(\tau+1)}L[f]ds}{\cosh c(s+\gamma_0)} \tag{24a}$$

where $\tanh\bar{c}\gamma_0 = 1/\overline{\rho c}$, $\overline{\rho c} > 1$ and

$$P(\tau) = P_0\bar{\rho}\,\frac{(\bar{c})^3}{\bar{B}}\cosh\bar{c}\gamma_0\,\frac{1}{2\pi i}\int_{-i\infty}^{i\infty}\frac{e^{s(\tau+1)}L[f]ds}{\sinh\bar{c}(s+\gamma_0)} \tag{24b}$$

when $\tanh\bar{c}\gamma_0 = \overline{\rho c}$, $\overline{\rho c} < 1$. The integrals in Eqs. (24a) and (24b) can be evaluated by expanding either $1/\cosh z$ or $1/\sinh z$ in powers of e^{-2z}.

from which we see that Eq. (24) is a series of modulated step functions separated in time by $2\bar{c}n$. These represent reflections inside the inclusion.

Integrals of the form Eq. (24) may be found in a table of inverse Laplace transforms.[6,11] Finally we have, for small-time response,

Case 1 ("soft" inclusion): $\overline{\rho c} > 1$

$$P(\tau) = P_0\bar{\sigma}\,\frac{(\bar{c})^3}{\bar{B}}\,2\sinh\bar{c}\gamma_0\sum_{n=0}^{\infty}(-1)^n\,e^{-(2n+1)\bar{c}\gamma_0}$$

$$f[\tau+1-(2n+1)\bar{c}]u[\tau+1-(2n+1)\bar{c}] \qquad (25a)$$

Case 2 ("hard" inclusion): $\overline{\rho c} < 1$

$$P(\tau) = P_0\bar{\sigma}\,\frac{(\bar{c})^3}{\bar{B}}\,2\cosh\bar{c}\gamma_0\sum_{n=0}^{\infty}e^{-(2n+1)\bar{c}\gamma_0}$$

$$f[\tau+1-(2n+1)\bar{c}]u[\tau+1-(2n+1)\bar{c}] \qquad (25b)$$

where $u(\tau)$ is the unit step function.

These expressions are applied to a few examples as shown in Figs. 8, 9, and 10 for the case of an incident step pressure. For Case 1 ($\overline{\rho c} > 1$) the inclusion acts as an "underdamped" transducer (Figs. 9 and 10) and as an "overdamped" transducer for Case 2 ($\overline{\rho c} < 1$) (Fig. 8). The damping is due, of course, to the fact that part of the reflected waves is radiated out of the inclusion into the matrix.

If we try to extend Eq. (25) for large time for the case of the step input, we obtain in both cases

$$P(\tau) = \frac{\bar{c}^2}{\bar{B}}\,P_0 \qquad (26)$$

where we have used the fact that

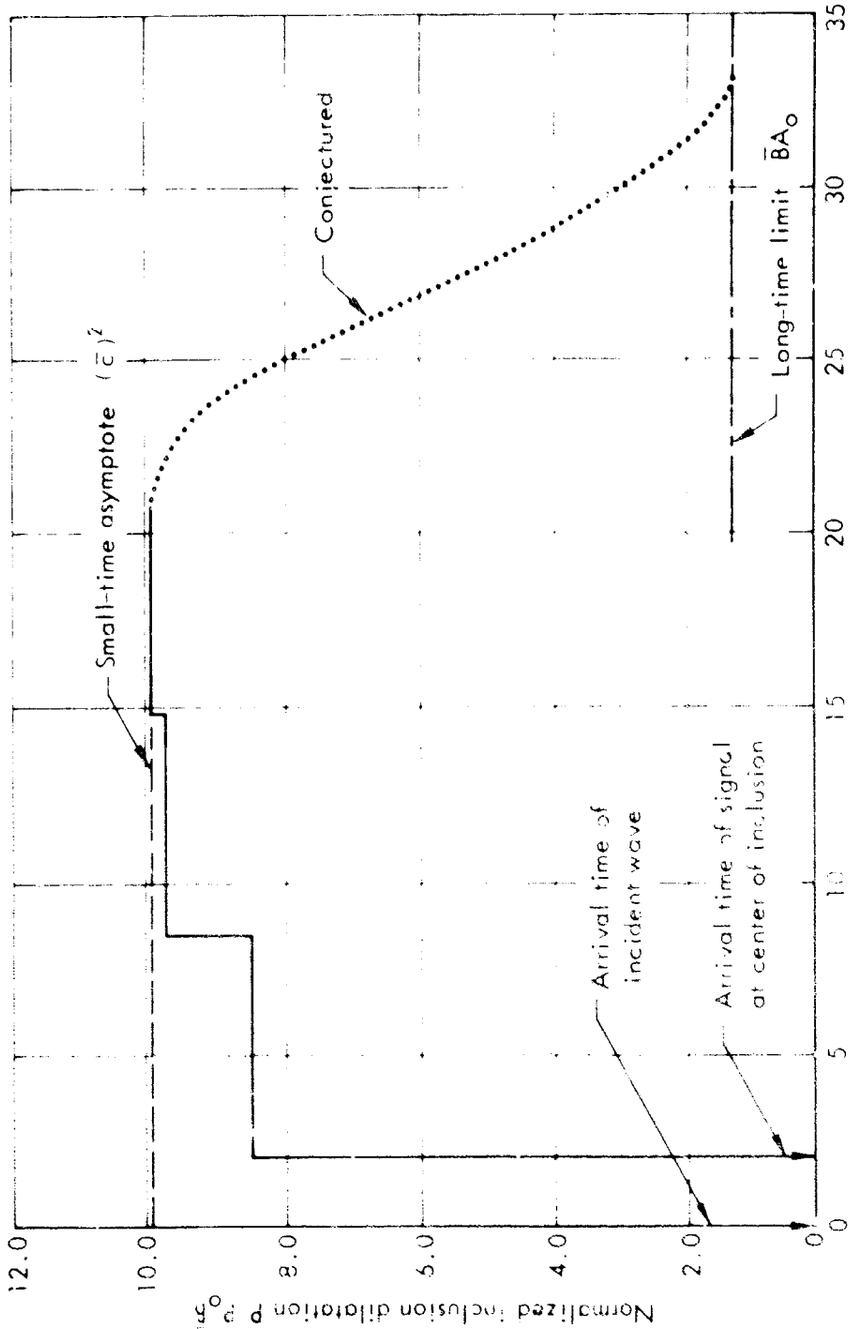

Fig. 3 — Dilatation versus time for a small-time transient response of lead inclusion in a granite matrix for an incident compressional step wave; decay of internal reflections

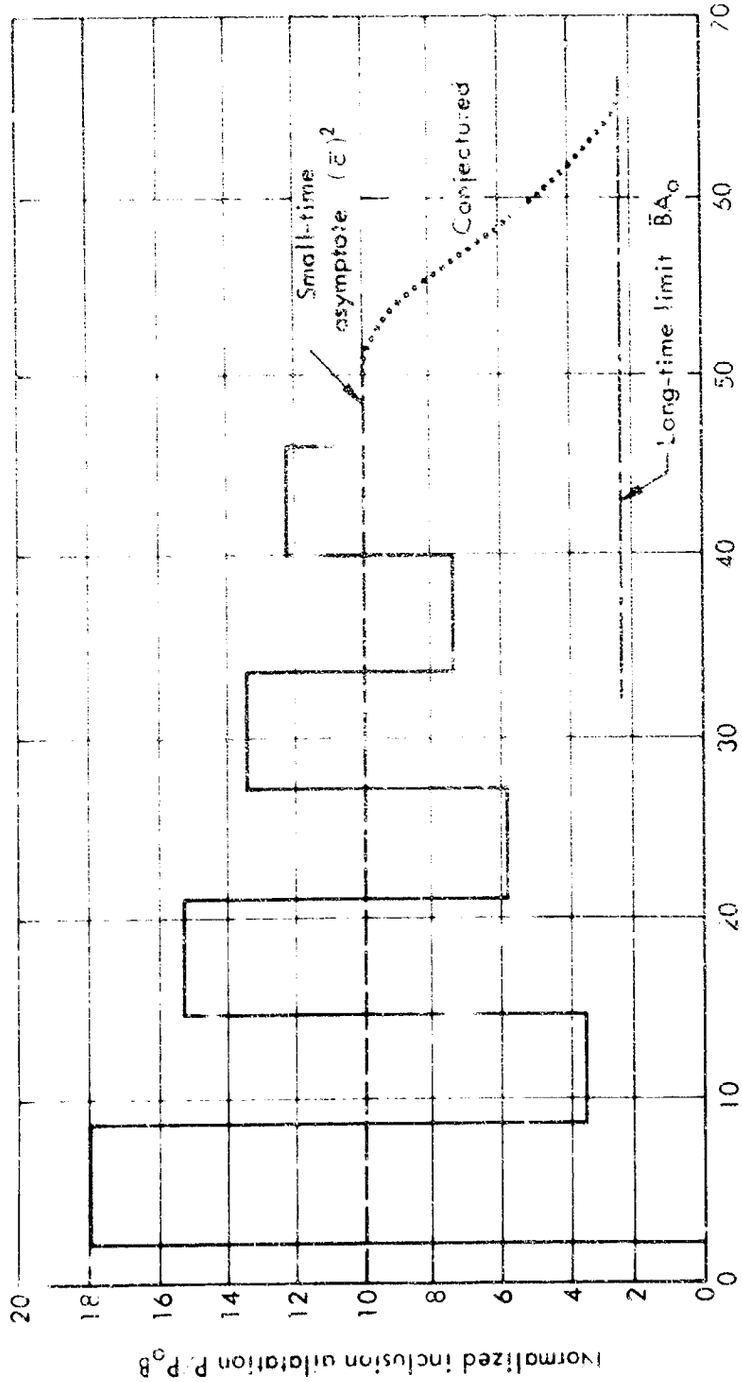

Fig. 9—Dilatation versus time for a small-time transient response of polyethylene inclusion in a granite matrix for an incident compressional step wave; decay of internal reflections

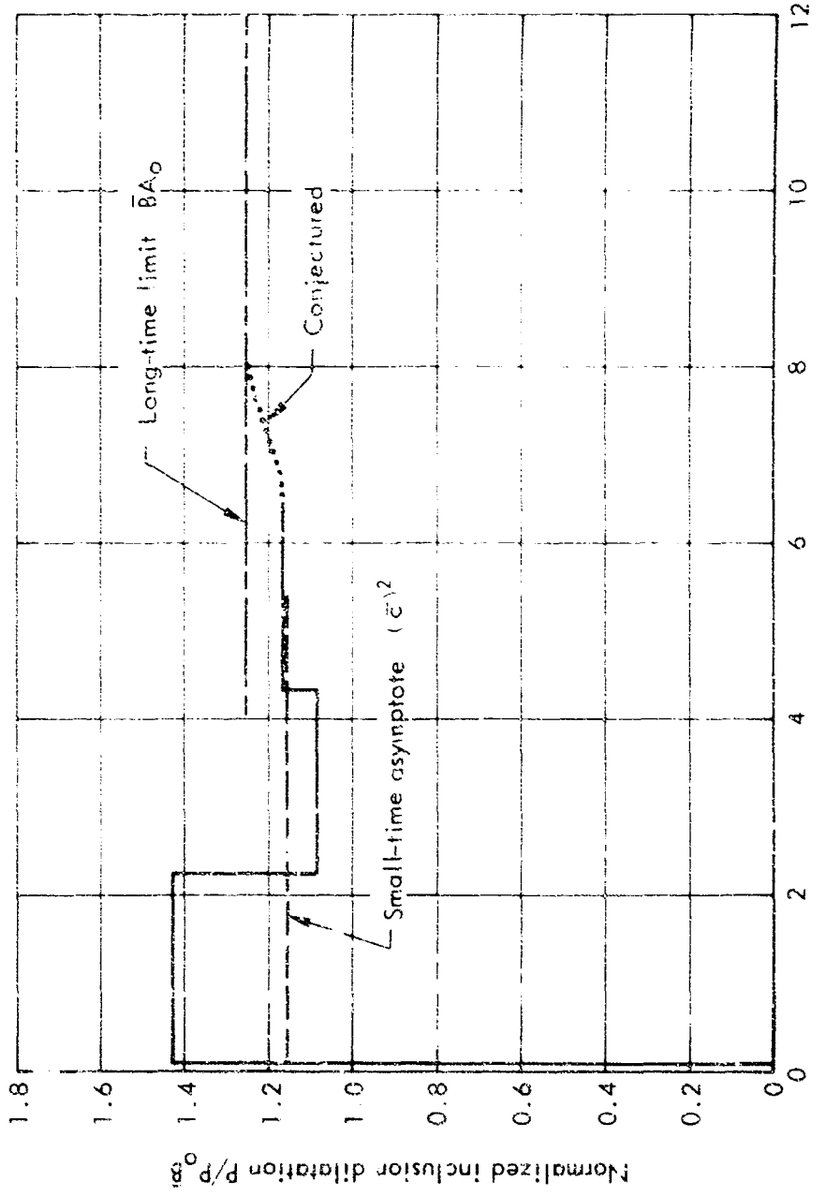

Fig. 10—Dilatation versus time for a small-time transient response of magnesium inclusion in a granite matrix for an incident compressional step wave; decay of internal reflections

$$2\sum_{n=0}^{\infty} e^{-(2n+1)\bar{c}\gamma_0} = \frac{1}{\sinh \bar{c}\gamma_0}, \qquad 2\sum_{n=0}^{\infty} (-1)^n e^{-(2n+1)\bar{c}\gamma_0} = \frac{1}{\cosh \bar{c}\gamma_0}$$

Thus, for the step input the short-time asymptote given by Eq. (26) using the approximation Eq. (23) differs from the long-time approximation Eq. (22) by a constant. This difference will be discussed shortly. The above factor represents the asymptotic maximum (minimum) in the frequency response for the case $\overline{\rho c} < 1$ ($\overline{\rho c} > 1$).

For the case $\overline{\rho c} > 1$

$$P \equiv \frac{\bar{c}^2}{\bar{B}}\left(2 \cosh \bar{c}\gamma_0 e^{-\bar{c}\gamma_0} - 1\right) = \frac{\bar{c}^2}{\bar{B}} e^{-2\bar{c}\gamma_0}$$

is a measure of the amount of overshoot for early time.

We see that this formulation has the advantage over the Fourier representation Eq. (18), since for a given time Eq. (25) contains a finite number of terms. In the latter expression $1/\bar{c}\gamma_0$ again plays the role of a "transient damping" time.

For the case of equal impedances $\overline{\rho c} = 1$, we return to the expression Eq. (18). The small-time expression is given simply by

$$P(\tau) = \frac{\bar{c}^2}{\bar{B}} P_0 f(\tau + 1 - \bar{c})$$

The small-time solution is exactly analogous to the penetration of a compressional wave into an infinite acoustic barrier of material different from that of the matrix and normal to the incoming wave. For that problem, if the acoustic impedance ratio is unity, there are no reflections, but rather a delay in the signal, which is what we found previously.

IV. THE SOLUTION OF THE INVERSE PROBLEM

While the goal of the analyst is to predict the output or response of a transducer given the input, the object of the experimentalist is the reverse. That is, the latter wishes to solve the inverse problem of finding the input given the output of the transducer.*

THE METHOD OF FOURIER TRANSFORM

Returning to Eq. (14), we write an expression for the free-field pressure P_c in terms of the mean pressure P at the origin of the inclusion

$$P_c(\tau) = \frac{\bar{B}}{\bar{c}} \frac{1}{2\pi} \int_{-\infty}^{\infty} e^{-i\alpha(\tau-1)} F[P]$$

$$\times \left\{ \frac{1}{\bar{\rho}\bar{c}} (-i)(\alpha + i) j_0(\bar{c}\alpha) - \left[\frac{4(1 - \bar{\mu})}{\bar{\mu} k_1^2} (\alpha + i) + i\alpha^2 \right] j_1 \frac{(\bar{c}\alpha)}{i\alpha} \right\} d\alpha \tag{27}$$

One may readily perform this inversion if the integral form of $j_n(z)$[6] is used, i.e.,

$$j_0(\bar{c}\alpha) = \frac{1}{2} \int_{-1}^{1} e^{i\bar{c}\alpha t} dt$$

$$j_2(\bar{c}\alpha) = -\frac{1}{4} \int_{-1}^{1} e^{i\bar{c}\alpha t} (3t^2 - 1) dt$$

and if

$$3j_1(z) = z\left[j_0(z) + j_2(z) \right]$$

The inversion is performed by switching the order of integration and making the necessary assumptions of integrability. Thus

*See Ref. 11 for an example from quantum mechanics.

$$P_c(\tau) = \frac{\bar{B}}{2\bar{c}} \int_{-1}^{1} \frac{1}{\bar{\rho}\bar{c}} \left[\frac{dP}{d\tau}(\tau - 1 - \bar{c}t) + P(\tau - 1 - \bar{c}t)\right] dt$$

$$- \frac{\bar{B}}{4} \int_{-1}^{1} \left\{\frac{4(1-\bar{\mu})}{\bar{\mu}k_1^2} \left[\frac{dP}{d\tau}(\tau - 1 - \bar{c}t)\right.\right.$$

$$\left.\left. + P(\tau - 1 - \bar{c}t)\right] - \frac{d^2P}{d\tau^2}(\tau - 1 - \bar{c}t)\right\}(1 - t^2)dt$$

Integrating by parts and collecting terms, the above expression assumes the form

$$P_c(\tau) = \frac{\bar{B}}{2(\bar{c})^2} \left[\left(1 + \frac{1}{\bar{\rho}\bar{c}}\right) P(t - 1 + \bar{c}) + \left(1 - \frac{1}{\bar{\rho}\bar{c}}\right) P(\tau - 1 - \bar{c})\right.$$

$$\left. - \left(1 - \frac{1}{\bar{\rho}}\right) \frac{1}{\bar{c}} \int_{-\bar{c}}^{\bar{c}} P(\tau - 1 - s)ds\right]$$

$$+ \frac{\bar{B}(1-\bar{\mu})}{(\bar{c})^3 \bar{\mu}k_1^2} \int_{-\bar{c}}^{\bar{c}} (s^2 + 2s - \bar{c}^2) P(\tau - 1 - s)ds \qquad (28)$$

Note that if $\bar{\mu} = \bar{c} = \bar{B} = \bar{\rho} = 1$, we obtain the identity $P_0(\tau) = P(\tau)$. For long time or $\tau - 1 >> 2\bar{c}$, we may remove $P(\tau - 1 - s)$ from the integrands and

$$P_c(\tau) \to \frac{\bar{B}}{\bar{c}} \left[\frac{1}{\bar{\rho}\bar{c}} - \frac{4}{3} \frac{(1-\bar{\mu})}{\bar{\mu}k_1^2} \bar{c}\right] P(\tau - 1) = A_0^{-1} P(\tau - 1) \qquad (29)$$

which is what we obtained for the direct problem, Eq. (22).

It is interesting to note that Mow[5] found an exact expression for the inverse problem of a rigid sphere. However in that problem the incident displacement U_c was found in terms of derivatives of U as well as an integral. Equation (28) involves only weighted integrals for the incident stress. This operation could be built into an electronic "black

box." The recorded signal $P(\tau)$, considered as an input, could be delayed and integrated electronically to produce an output proportional to the original incident pressure. The operations in Eq. (28) thus decode the transducer output.

The solution of the inverse problem for the center pressure was possible because $C_0^{-1}(\omega)$ in Eq. (6) was a linear combination of spherical Bessel functions. No such simple relation results for the shear stress S, Eq. (6), or the displacement of the center of mass $\langle \underline{U} \rangle$, Eq. (7).

THE METHOD OF SUCCESSIVE REFLECTIONS

Having obtained an exact expression for the incident pressure $P_c(\tau)$ in terms of the center pressure in the inclusion, we can then look at Eq. (28) as an integral equation for $P(\tau)$ in terms of the incident pressure. We will in fact show that by this method an exact solution for $P(\tau)$ can be obtained by a finite time, step-by-step algorithm.

To begin, we shift the time by

$$\tau_1 \equiv \tau - 1 + \bar{c} \quad \text{and} \quad \eta \equiv \tau_1 - \bar{c} - s$$

so that Eq. (28) takes the form

$$P_c(\tau_1 + 1 - \bar{c}) = \frac{\bar{B}}{2(\bar{c})^2}\left[\left(1 + \frac{1}{\bar{\rho}\bar{c}}\right)P(\tau_1) + \left(1 - \frac{1}{\bar{\rho}\bar{c}}\right)P(\tau_1 - 2\bar{c})\right.$$

$$\left. - \left(1 - \frac{1}{\bar{\rho}}\right)\frac{1}{\bar{c}}\int_{\tau_1 - 2\bar{c}}^{\tau_1} P(\eta)\,d\eta\right]$$

$$+ \frac{\bar{B}}{(\bar{c})^3}\,\frac{(1-\bar{\mu})}{\bar{\mu}k_1^2}\int_{\tau_1 - 2\bar{c}}^{\tau_1} P(\eta)\left[(\tau_1 - \eta - \bar{c})^2\right.$$

$$\left. + 2(\tau_1 - \eta - \bar{c}) - \bar{c}^2\right]d\eta$$

We assume that the center pressure is zero until $\tau_1 = 0$, or that the incident pulse arrives at the origin at time $\tau_1 = 1 - \bar{c}$. These conditions imply the following:

$$P(\tau_1) = 0 \qquad \tau_1 < 0$$

$$P_c(\tau_1) = 0 \qquad \tau_1 < 1 - \bar{c}$$

$$P(\tau_1 - 2\bar{c}) = 0 \qquad \tau_1 < 2\bar{c}$$

$$\int_{\tau_1 - 2\bar{c}}^{0} P(\eta)d\eta = 0$$

Since $\bar{c}$ is the half transit time in the inclusion, the center of the inclusion does not see an internal reflection until time $\tau_1 = 2\bar{c}$. Thus for $0 \leq \tau_1 \leq 2\bar{c}$,

$$P_c(\tau_1 + 1 - \bar{c}) = \frac{\bar{B}}{2(\bar{c})^3}\left[\bar{c}\left(1 + \frac{1}{\bar{\rho}\bar{c}}\right)P(\tau_1) + \int_0^{\tau_1} K(\tau_1 - \eta)P(\eta)d\eta\right] \qquad (30)$$

where

$$K(\tau_1 - \eta) \equiv \frac{(1 - \bar{\mu})}{\bar{\mu}k_1^2}\left[(\tau_1 - \eta - \bar{c})^2 + 2(\tau_1 - \eta - \bar{c}) - \bar{c}^2\right] - \left(1 - \frac{1}{\bar{\rho}}\right)$$

This is an integral equation of the Volterra kind. Since $K(\tau_1 - \eta)$ is a polynomial, Eq. (30) may be solved by successively differentiating it with respect to τ_1, using the identity

$$\frac{d}{d\tau_1}\int_0^{\tau_1} K(\tau_1 - \eta)P(\eta)d\eta = K(0)P(\tau_1) + \int_0^{\tau_1} \frac{\partial}{\partial\tau_1} K(\tau_1 - \eta)P(\eta)d\eta$$

This results in an ordinary linear differential equation with constant coefficients for $P(\tau_1)$, with initial conditions determined at each differentiation of Eq. (30), i.e.,

$$\dddot{P}_c(\tau_1 + 1 - \bar{c}) = \frac{\bar{B}}{2(\bar{c})^3}\left[\bar{c}\left(1 + \frac{1}{\bar{c}\rho}\right)\dddot{P}(\tau_1) + K(0)\ddot{P}(\tau_1)\right.$$

$$\left. + K'(0)\dot{P}(\tau_1) + K''(0)P(\tau_1)\right] \tag{31}$$

with

$$P_c(1 - \bar{c}) = \frac{\bar{B}}{2(\bar{c})^2}\left(1 + \frac{1}{\bar{\rho}\bar{c}}\right)P(0^+) \tag{31a}$$

$$\dot{P}_c(1 - \bar{c}) = \frac{\bar{B}}{2(\bar{c})^3}\left[\bar{c}\left(1 + \frac{1}{\bar{c}\rho}\right)\dot{P}(0^+) + K(0)P(0^+)\right] \tag{31b}$$

$$\ddot{P}_c(1 - \bar{c}) = \frac{\bar{B}}{2(\bar{c})^3}\left[\bar{c}\left(1 + \frac{1}{\bar{c}\rho}\right)\ddot{P}(0^+) + K(0)\dot{P}(0^+) + K'(0)P(0^+)\right] \tag{31c}$$

For our problem

$$K(0) = \left(\frac{1}{\bar{\rho}} - 1\right) - \frac{2(1 - \bar{\mu})\bar{c}}{\bar{\mu}k_1^2}$$

$$K'(0) = \frac{2(1 - \bar{\mu})}{\bar{\mu}k_1^2}(1 - \bar{c})$$

$$K''(0) = \frac{2(1 - \bar{\mu})}{\bar{\mu}k_1^2}$$

The solution consists of a particular solution determined by $\dddot{P}_c(\tau_1 + 1 - \bar{c})$ and a transient solution of the form

$$P(\tau_1) = \sum_{j=1}^{3} a_j e^{i\beta_j \tau_1} \qquad 0 < \tau_1 < 2\bar{c} \tag{32}$$

where the roots of the following algebraic equation are represented by β_j:

$$c\left(1 + \frac{1}{\overline{\overline{c\rho}}}\right)(i\beta)^3 + K(0)(i\beta)^2 + K'(0)(i\beta) + K''(0) = 0 \qquad (33)$$

The three constants a_j are determined by the initial conditions, Eqs. (31a), (31b), and (31c).

Once the solution is known in the interval $0 < \tau_1 \leq 2\bar{c}$, the solution may be extended into the interval $2\bar{c} < \tau_1 \leq 4\bar{c}$, since $P(\tau_1 - 2\bar{c})$ will be known, as will

$$\int_{\tau_1 - 2\bar{c}}^{2\bar{c}} P(\eta) K(\tau_1 - \eta) d\eta$$

A comparison between the solutions obtained in Eq. (21) (method of residues) and Eq. (32) (method presented here) reveals a difference in the number and magnitude of eigenvalues present in each. In Eq. (32), there exists a finite number β_j; in Eq. (21), there is an infinite number α_j. This can be explained by the fact that the two forms of the solution are valid over different time domains. Equation (21) is valid for all time and must contain information about the periodic discontinuities in pressure due to reflections. The method discussed here obtains a solution, Eq. (32), valid only between reflections ($2n\bar{c} \leq \tau_1 < 2(n + 1)\bar{c}$) and continuous in these intervals as long as $\ddot{\overline{P}}_c$ is continuous.

We may note that this method may be applied to the conversion of certain integrals of the form

$$f(t) = \frac{1}{2\pi} \int_{-\infty}^{\infty} \frac{e^{-i\alpha t} H(\alpha) d\alpha}{\sum_{n=-M}^{N} \alpha^n g_n(\alpha)}$$

where

$$H(\alpha) = \int_{-\infty}^{\infty} e^{i\alpha t} h(t) dt$$

and the $g_n(\alpha)$ are periodic functions and bounded. One must also assume that $\sum_{n=-M}^{N} \alpha^n g_n(\alpha) = 0$ has no roots on the real axis.

V. SUMMARY OF RESPONSE CHARACTERISTICS

We now recapitulate the main results of the various methods used to analyze the response of an embedded elastic spherical transducer.

1. The pressure or mean stress response at the center of the inclusion will be independent of the orientation of the inclusion relative to the wave front and will only depend on the spherically symmetric modes, as shown in Eq. (6).

2. The pressure response at the center of the inclusion will not depend on whether the incident wave is plane or spherical. The stress τ_{zz}, however, will be sensitive to the spherical character of the wave front.

3. The higher free spherical vibrational modes of an embedded inclusion are characterized by commensurable frequencies and radiation damping independent of frequency.

4. The rate of decay of internal reflections will depend on the impedance ratio $\bar{\rho}\bar{c}$ and will have a characteristic time γ_0^{-1} given by Eqs. (20a) or (20b) (see Table 1).

5. The pressure response for small time is characterized by behavior which is either "underdamped" (Eq. (25a)) or "overdamped." For the former, the overshoot above the small-time asymptote is given by $(\bar{c})^2 e^{-2\bar{c}\gamma_0}/\bar{B}$ for an incident step wave (see Table 1).

6. The inverse problem may be solved for the incident pressure in terms of the pressure at the center of an embedded inclusion, from which an exact solution may be obtained for the direct problem by a reflection-by-reflection method. This is not possible for either the displacement of the center of mass (except for a rigid inclusion) or the shear stress at the center.

Furthermore, we will make some comments on the difference between the small-time asymptote and the large-time behavior for a step input. When the incident wave encounters the inclusion at $\tau = -1$, the internally transmitted compressional wave at normal incidence to the surface will reach the center first at $\tau = \bar{c} - 1$, reflect at the leeward surface, and return to the center at $\tau = 3\bar{c} - 1$. The expression Eqs. (25a) or (25b) essentially only treats the response from this normal-incidence

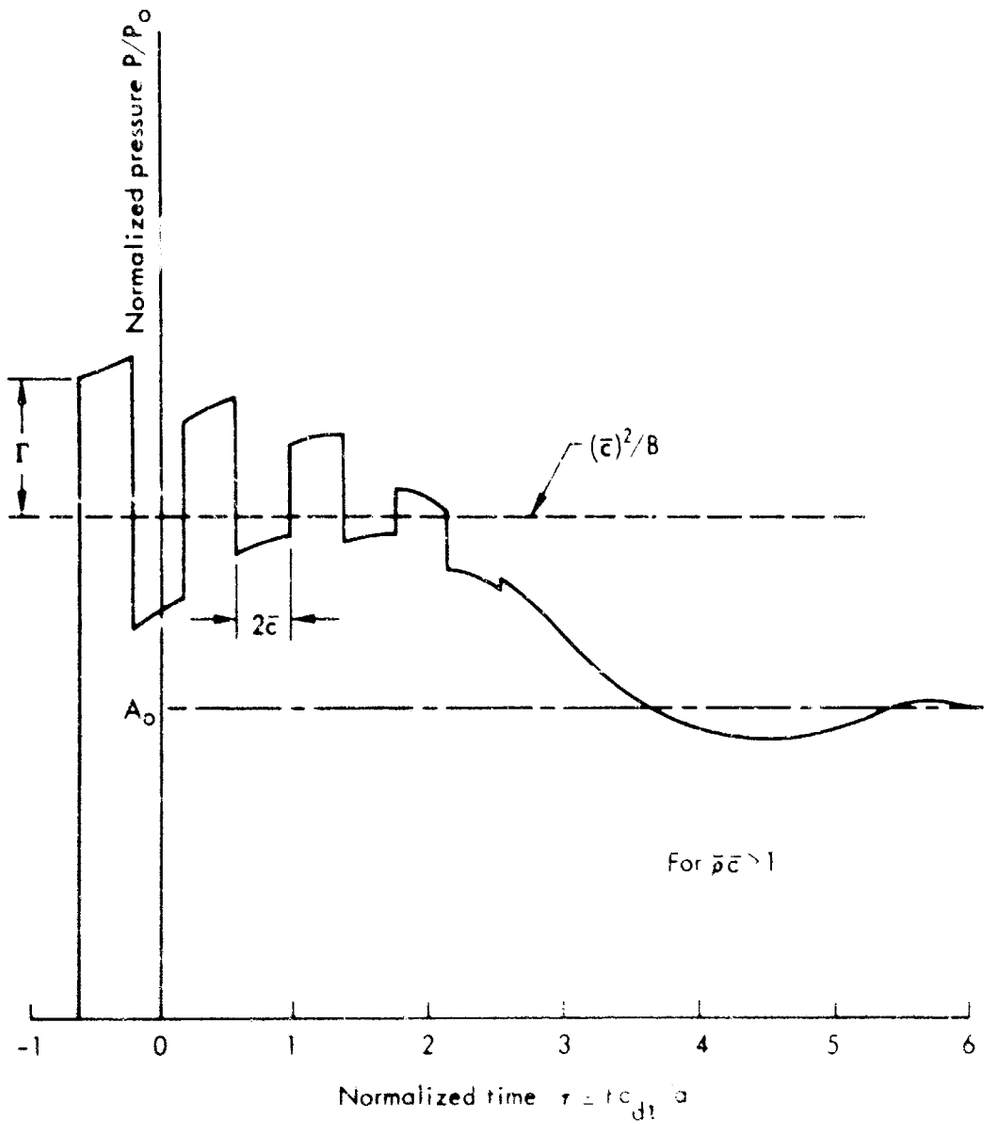

Fig. 11 — Conjecture on the qualitative response of an embedded inclusion due to an incident compressional step wave

wave and neglects the shear-mismatch-induced waves ($\bar{\upsilon} \neq 1$) when the incident wave is oblique to the spherical surface. Thus the reflections in Figs. 8, 9, and 10 probably do not give the total response after one or two reflections, except if $\bar{c} \ll 1$. If we may be permitted to conjecture, the total response of the pressure at the center of the inclusion for a step input may resemble Fig. 7 for $\bar{c} \sim 0(1)$. The small-time overshoot and large-time overshoot may be useful as guides to designing such a pressure transducer or interpreting the results of an actual test.

Finally, we should mention that actual materials have internal friction or damping properties which were neglected here. To include these properties, the elastic moduli can be replaced by the complex counterparts as a function of frequency in Eq. (14). Material attenuation of sound waves would be important in a transducer made of plastic, e.g., polyethylene (Figs. 4 and 9), and in fact might be desirable.

VI. ON THE DESIGN OF A STRESS-STRAIN TRANSDUCER

At the beginning of this Memorandum we outlined the important characteristics that a stress-strain transducer should have. In the subsequent sections we analyzed the transient response of a spherical pressure transducer and discovered the parameters that affect the response characteristics. We propose here to describe one possible design for such a transducer, which may serve as a point of reference for all apparent areas of field testing, with the possible exception of ground-shock testing.

OVERALL DESIGN CONCEPT

The proposed stress transducer will sense the pressure in a ground-shock environment by measuring the deformation, or average strain at the center of a spherical elastic inclusion by means of strain gages. The sphere is to be bonded to a cylindrical sample of the ground material and grouted in a bore hole (Fig. 12). The spherical shape and choice of average strain will result in a transducer insensitive to orientation relative to the wave front and curvature of the wave front.

This unorthodox shape may create some fabrication problems. Several alternatives are available. The sphere may be split into hemispheres, the gages installed, and the sphere fastened or cemented together. This, however, might destroy the spherical symmetry of its response. If the inclusion material has a low melting point or can be solidified from the liquid state at low or room temperatures (e.g., epoxy), the gages might then be directly embedded in the sphere before solidification. This method, although attractive, will usually mean a large mismatch in acoustic impedance ρc between inclusion and matrix, and hence large internal reflections and a long transient decay time. Under certain circumstances a large impedance mismatch might be preferred, especially in high pressure shocks where the pressure in the inclusion would be attenuated below the fracture limit by the choice of a soft material such as plastic or lead.

A third alternative, the one preferred here, is to drill small radial access holes through the center and to cement semiconductor

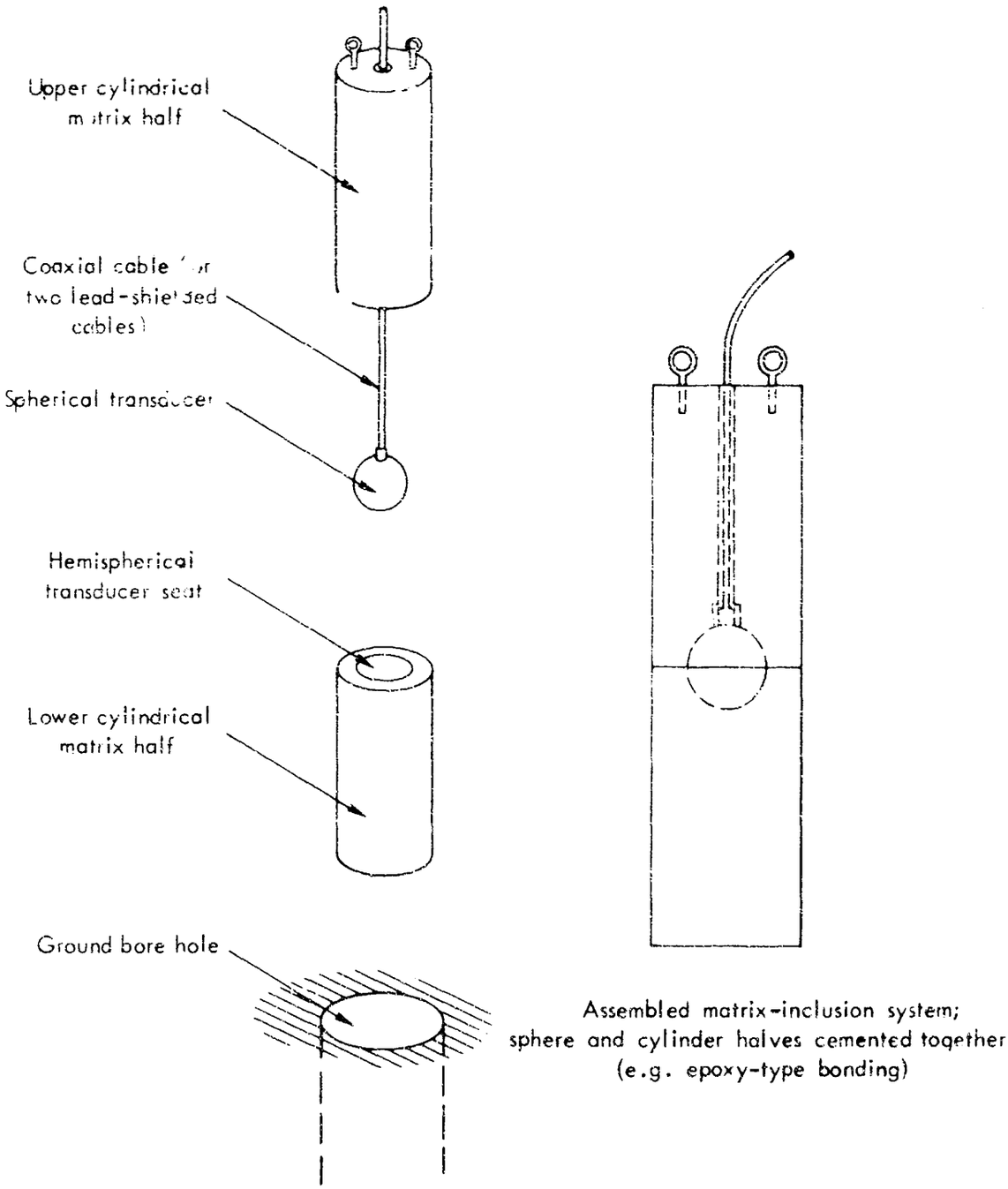

Fig. 12 — Installation details of the cylindrical matrix - spherical transducer assembly

strain gages along the axis of the cylindrical hole several hole diameters away from the center, thereby avoiding stress concentration effects due to the tri-hole intersection. If the access-hole diameter is small compared with the inclusion radius, diffraction effects should be small. Frequency response, however, will be limited by the acoustic impedance ratio and inclusion radius rather than the gage-hole diameter.

MATERIAL, STRENGTH, AND SIZE REQUIREMENTS

To minimize the spurious transients in the transducer which are due to internal reflections, the inclusion material should be chosen so that its acoustic impedance is as close as possible to that of the ground matrix. For example, in a granite matrix (Table 1) aluminum would be the best choice for inclusion material to minimize overshoot and reflections.

In regard to the required strength of the transducer, it should be remembered that the pressure at low frequencies in the inclusion may be higher or lower than that in the free field. For a granite matrix $P/P_0(\omega \to 0) = 1.4$ for a steel inclusion, $P/P_0 = 1.3$ for titanium, and $P/P_0 = 0.81$ for magnesium. Thus, while a magnesium inclusion can support a matrix pressure 24 percent above its fracture strength, a steel inclusion can support a matrix measure only 72 percent of its fracture strength.

The size of the device is limited by the seismic bore hole, the size of the strain-gage access holes, and the desired frequency response.

There are two "figures of merit" for the transient response. One is the rise time or time to transient decay due to a step input, the other is the frequency response as determined from the pressure ratio versus wave number or frequency curves (Figs. 2 through 5). The rise time or transient damping time is independent of the size and depends only on the acoustic impedance ratio of matrix and inclusion.

The frequency response is usually defined by the frequency at which the gain $A(\omega) \equiv P/P_0$ is up or down 3 dB ($dB \equiv 20 \log_{10} A$) or where $A = 1.41$ or 0.71. This frequency will depend on the radius of the inclusion. For a lead inclusion (4-in. diameter) in a granite matrix, the

gain or pressure ratio P/P_0 will be up 3 dB when the frequency is around 10,000 cycles/sec. For a titanium inclusion the frequency response is around 0 - 47 kc/sec for a 4-in. diameter inclusion. This 3-dB figure may be a little misleading, since the whole response for titanium never varies more than about 4 dB (Fig. 5), and for aluminum (upper curve Fig. 2), never more than 3 dB. It is far easier to extend the frequency response by matching the acoustic impedance than by making the inclusion smaller.

STRAIN GAGES AND ELECTROMAGNETIC INTERFERENCE

The strain sensors for this transducer are semiconductor strain gages. These piezoresistive cylindrical elements[12] would be cemented in pairs along each of the three mutually perpendicular axes of the access holes (Fig. 13). The gages would be mounted on each side of the center of the sphere at a distance of four hole diameters away from the center to avoid stress concentration effects near the center. Each pair would be connected in series, and the three pairs then series-connected into a total of six gages forming one arm of a wheatstone bridge. The output of the bridge would be proportional to twice the dilatation; hence the pressure at the center of the sphere.

If transient electromagnetic radiation is a problem, the gages may be isolated from the sphere which, if a conductor, will check the intrusion of electromagnetic radiation into the interior through the skin effect. All but quasistatic fields would be shielded from the strain gages.

FABRICATION AND INSTALLATION

The small size of the gage-access holes will, of course, present some fabrication problems. However, the use of specially designed tweezers and probes and a low-powered microscope should make the problem tractable. Small-diameter enamel-coated lead wire should be threaded through the holes before installing the gages. The gages can be connected in pairs and installed as such, so that all the leads exit from only one access hole. With the leads soldered as one arm of a bridge,

Note:
Gages ①-②-③-④-⑤-⑥ connected in series
Output: Two leads to external bridge

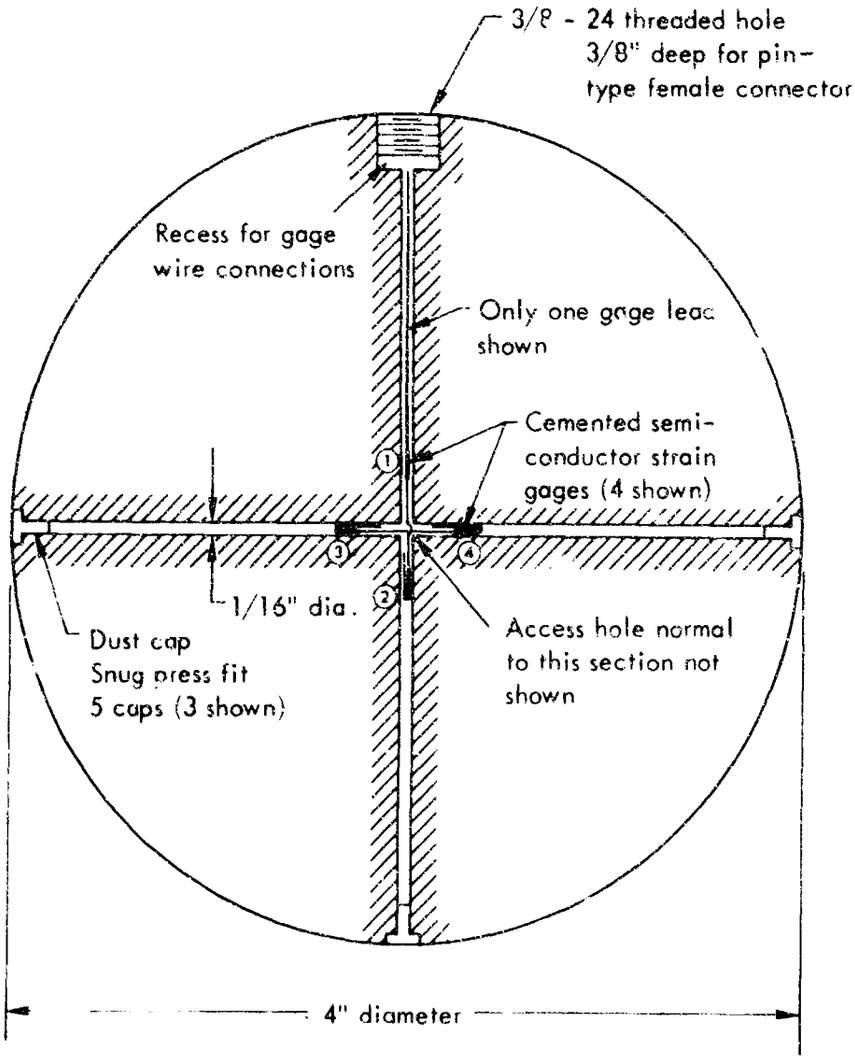

Fig. 13 – Hemispherical section of a spherical pressure transducer

only two leads need be carried back to a ground station into a bridge through a coaxial or shielded cable. If electromagnetic radiation is not a problem, one of the leads may be grounded to the sphere itself.

An exploded diagram of the installed transducer is shown in Fig. 12. Rather than simply grouting the sphere in place with loose ground material, we suggest a cylindrical sample of the ground be obtained if possible and split into two smaller cylinders. On one of the ends of each cylinder a hemispheric hole would be machined to fit the sphere. Through one of the cylinders, a small axial hole would be needed for the transducer cable. The two halves would then be cemented (with some epoxy, for example) to the sphere. The transducersphere in the cylindrical matrix would then be lowered into the seismic bore hole and grouted.

There are of course many other factors to consider in properly designing an instrumentation system. Some of these, such as the auxiliary electronic equipment, are beyond the scope of this study and the experience of its authors. However, no proper evaluation of the problems can begin without a specific device at hand with concrete sizes and specifications; we have attempted to provide these numbers and properties for those with intimate knowledge and experience in field testing.

The overall advantage of this design is not lower cost or ease of installation (though that may be true), but that its shape, internal construction, and installation allow the response and field results to be directly compared with a theoretical analysis. The output of the transducer can be systematically decoded to determine the pressure in the incident wave field.

REFERENCES

1. Simmon, K. B., *Dynamic Rock Instrumentation Survey*, Air Force Weapons Laboratory, Kirtland Air Force Base, New Mexico, Report TR-68-3, 1968.

2. Ying, C. F., and R. Truell, "Scattering of a Plane Longitudinal Wave by a Spherical Obstacle in an Isotropically Elastic Solid," *J. Appl. Phys.*, Vol. 27, No. 7, September 1956, p. 1086.

3. Pao, Yih-Hsing, and C. C. Mow, "Scattering of Plane Compressional Waves by a Spherical Obstacle," *J. Appl. Phys.*, Vol. 34, No. 3, March 1963, pp. 493-499.

4. Mow, C. C., *On the Effects of Stress-Wave Diffraction on Ground-Shock Measurements: Part I*, The RAND Corporation, RM-4341-PR, January 1965.

5. Mow, C. C., and T. Repnau, *On the Effects of Stress-Wave Diffraction on Ground-Shock Measurements: Part II*, The RAND Corporation, RM-4556-PR, July 1965.

6. Morse, P. H., and H. Feshbach, *Methods of Mathematical Physics*, McGraw-Hill Book Co. Inc., New York, 1953.

7. Timoshenko, S., and J. N. Goodier, *Theory of Elasticity*, McGraw-Hill Book Co. Inc., New York, 1951, p. 359.

8. Clark, S. P. (ed.), *Handbook of Physical Constants*, Geological Society of America, New York, 1966.

9. Papoulis, A., *The Fourier Integral and Its Applications*, McGraw-Hill Book Co. Inc., New York, 1962.

10. Skalak, R., and M. B. Friedman, "Reflection of an Acoustic Step Wave From an Elastic Cylinder," *J. Appl. Mech.*, Vol. 25, No. 1, March 1958, pp. 103-108.

11. Abramowitz, M., and L. A. Stegun (eds.), *Handbook of Mathematical Functions*, National Bureau of Standards, June 1964.

12. Baldwin-Lima-Hamilton Corporation, *Semiconductor Strain Gage Handbook*.

DOCUMENT CONTROL DATA

1. ORIGINATING ACTIVITY	2a. REPORT SECURITY CLASSIFICATION
THE RAND CORPORATION	UNCLASSIFIED
	2b. GROUP

3. REPORT TITLE

THE EFFECT OF STRESS-WAVE DIFFRACTION ON STRESS MEASUREMENTS AND A CONCEPT FOR AN OMNIDIRECTIONAL DYNAMIC STRESS GAGE

4. AUTHOR(S) (Last name, first name, initial)

Moon, D. C. and C. C. Mow

5. REPORT DATE	6a. TOTAL No. OF PAGES	6b. No. OF REFS.
January 1969	58	12

7. CONTRACT OR GRANT No.	8. ORIGINATOR'S REPORT No.
F44620-67-C-0045	RM-5860-PR

9a. AVAILABILITY/LIMITATION NOTICES	9b. SPONSORING AGENCY
DDC-1	United States Air Force Project RAND

10. ABSTRACT

An analysis of the transient response of the pressure in an embedded elastic inclusion due to an incident compressional wave. Also included in the study is an outline of a design for an omnidirectional pressure transducer with a response capable of being analyzed by the methods of the theory of elastic wave propagation and diffraction. The transducer proposed is an elastic spherical inclusion that is to be buried in the ground and is sensitive, through strain gages, to the mean stress or pressure at its origin. Both frequency response and transient behavior are treated. Two methods are given for determining total pressure response. One uses the calculus of residues and the high-frequency response and sums the resulting infinite series. The other solves the inverse problem by a Fourier transform method and finds the incident pressure in terms of the mean pressure at the center of the inclusion, for which an exact, explicit solution is found between successive reflections. The procedure could be used to decode the transducer output electronically.

11. KEY WORDS

Nuclear effects
Physics
Detection
Instrumentation